University of North Dakota
UND Scholarly Commons

Theses and Dissertations

Theses, Dissertations, and Senior Projects

2014

Geoneutrino production of the northern Black Hills, South Dakota, United States of America

Eric Eric Zimney
University of North Dakota

Follow this and additional works at: https://commons.und.edu/theses

Part of the Geology Commons

Recommended Citation

GEONEUTRINO PRODUCTION OF THE NORTHERN BLACK HILLS,
SOUTH DAKOTA, UNITED STATES OF AMERICA

by

Eric Gerald Zimny

A Thesis

Submitted to the Graduate Faculty

of the

University of North Dakota

In partial fulfillment of the requirements

for the degree of

Master of Science

Grand Forks, North Dakota
May
2014

This thesis, submitted by Eric Gerald Zimny in partial fulfillment of the requirements for the Degree of Master of Science from the University of North Dakota, has been read by the Faculty Advisory Committee under whom the work has been done, and is hereby approved.

_____
Dr .William Gosnold

_____
Dr. Ronald Matheney

_____
Dr. Kanishka Marasinghe

This thesis is being submitted by the appointed advisory committee as having met all of the requirements of the Graduate School at the University of North Dakota and is hereby approved.

_____
Wayne Swisher
Dean of the Graduate School

_____
Enter the Date

Title   Geoneutrino Production of the Northern Black Hills, South Dakota, United
               States of America.

Department   Geology & Geological Engineering

Degree   Master of Science

        In presenting this thesis in partial fulfillment of the requirements for a graduate
degree from the University of North Dakota, I agree that the library of this University
shall make it freely available for inspection. I further agree that permission for extensive
copying for scholarly purposes may be granted by the professor who supervised my
thesis work or, in his absence, by the Chairperson of the department or the dean of the
Graduate School. It is understood that any copying or publication or other use of this
thesis or part thereof for financial gain shall not be allowed without my written
permission. It is also understood that due recognition shall be given to me and to the
University of North Dakota in any scholarly use which may be made of any material in
my thesis.

                                                              Eric Gerald Zimny
                                                              04/23/2014

Table of Contents

LIST OF FIGURES

LIST OF TABLES

ACKNOWLEDGEMENTS

Megan Lonksi for always believing in me.

My committee and the professors of the UND geology department.

My fellow graduate students for providing a wonderful atmosphere.

ABSTRACT

Current neutrino observatories operate underground to isolate the detector from cosmic rays and background radiation. However, background radiation from local sources has yet to be accounted for. Current models for neutrino contributions from terrestrial rocks are formulated from bulk compositional estimates of the whole Earth. To better understand local background radiation from geologic sources surfaces rocks were collected throughout the area surrounding the Homestake Mine, South Dakota, home of the Sanford Underground Research Laboratory. The surface rocks were analyzed for radioactivity and neutrino luminosity, producing heat maps indicating the levels of neutrino production throughout the area. The area around the Homestake Mine was found to be more luminous then upper crustal averages generated from current bulk silicate Earth models.

CHAPTER I

INTRODUCTION

Neutrino physics experiments began in the 1960s with the installation of the first solar neutrino detector by Raymond Davis Jr and John N. Bahcall in the Homestake Mine, South Dakota. That experiment set out to collect and count neutrinos emitted by the Sun's process of nuclear fusion. The Homestake mine proved useful as an experiment location, as the thick overburden of rock provided a shield from other forms of radiation interference (Bahcall and Davis, 1988). This location continues to be of particular use to the scientific community today, and efforts were made to designate the Homestake Mine as an underground laboratory after its closure. In 2006 the property was donated to the State of South Dakota for use as an underground laboratory. Today the Homestake mine is home to the Sanford Underground Research Facility and currently operates dark matter and neutrino experiments. The underground lab is also being considered as a site for longer term experiments such as the Long Baseline Neutrino Experiment (LBNE) and a project called Dual Ion Accelerators for Nuclear Astrophysics (DIANA). The Homestake mine also provides an ideal location for a dedicated geoneutrino detector (Lesko, 2013).

The current generation of neutrino detectors exists in locations of opportunity; pre-excavated underground spaces originally commissioned for another purpose.

Two of these detectors, the Kamiokande detector in Japan, and the SNO+ detector in Ontario, Canada both reside in old mine excavations. Kamiokande is a large water Cherenkov detector constructed in 1991 and is operated by an international consortium of about 110 people and 30 institutes from Japan, the United States, Korea, China, Poland and Spain. SNO+ is a large liquid scintillator detector located on the north shore of Lake Huron outside Sudbury Ontario, Canada. The SNO+ project was proposed and is operated by a consortium of Canadian universities: Carleton University, Laurentian University, Queen's University, the University of British Columbia, the University of Guelph and the Universite de Montreal. The third detector, Borexino, is located in Italy and is operated by an international consortium as part of the Italian Institute for Nuclear Physics (INFN). A pre-existing research laboratory is primarily why the Sanford Underground Research Facility in the Homestake Mine is such a valued space for a dedicated neutrino detector experiment (About Us, 2014). Though the Homestake Mine presents an ideal space the question remains if the location is suitable from a geology standpoint. Local radioactivity within the northern Black Hills is unknown, and current geoneutrino flux estimates rely on bulk composition data. What is the geoneutrino production within the area of the Homestake Mine(Figure 1) (Figure 2)? Are there radioactive rocks in the area and how may their neutrino production affect experiments at the Sanford Underground Research Laboratory?

Figure 1. Map of South Dakota. The red pin indicates the location of the Homestake mine, and the northern Black Hills. Modified from the ArcGIS United States basemap

Figure 2. Map close up of the study area around Lead South Dakota overlain on the ArcGIS topographic basemap. The red pin indicates the location of the Homestake Mine

CHAPTER II

METHODS

Geoneutrino production was first hypothesized by Wolfgang Pauli in 1930 during early studies of the process of beta decay. Beta decay is a process through which a neutron becomes a proton and emits an electron and an antineutrino. Antineutrinos produced within the Earth are referred to as geoneutrinos. In the early studies of this process, before the existence of a neutrino was known, scientists studied the energy of the emitted electron (Reines and Cowan, 1994). A definite amount of energy was found to be released during radioactive decay, and the law of energy conservation requires that the released energy must be shared by the recoil nucleus and the electron. Using the law of energy conservation and that of conservation of momentum scientists of the time deduced that the electron should always carry away the same amount of energy. James Chadwick in 1914, however, demonstrated that the energy of the electron in beta decay was not a discrete value, but a continuous spectrum of energy (Reines and Cowan, 1994). When this continuous spectrum of energy was at its maximum the total energy before and after the reaction was the same, and energy was conserved. However, in all other examples some of the energy was lost. This is where Wolfgang Pauli's hypothesis filled in the gap: that a yet undiscovered particle, originally dubbed the neutron and later renamed as the neutrino by Enrico Fermi, may also be emitted.

This newly discovered particle, the neutrino, would carry away the unaccounted for energy and satisfy the laws of energy conservation and the conservation of momentum (Reines and Cowan, 1994). Enrico Fermi's work regarding the weak force solidified the idea of the neutrino and gave scientists a way to test for the presence of the particle. Shortly after Fermi's work regarding the neutrino was finished Hans Bethe and Rudolf Peierls theorized a reaction in which a free neutrino would interact with matter and be stopped, allowing for its detection (Bethe and Bacher, 1936). This reaction is demonstrated by equation 1 below.

Equation 1:

$$\bar{v} + N\,(n, p) \rightarrow e^+ + N\,(n + 1, p - 1)$$
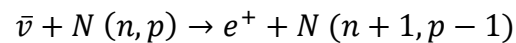
Where *n* equals the number of neutrons and *p* equals the number of protons. A simplified version of this equation deals with a neutrino interaction with hydrogen demonstrated by equation 2.

Equation 2:

$$\bar{v} + p \rightarrow n + e^+$$
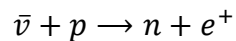
This theorized reaction takes place when a free antineutrino strikes a proton inducing what is termed inverse beta decay. In inverse beta decay the neutrino strikes the proton and becomes a positron while the proton in the reaction becomes a neutron. Shortly after the reaction takes place the positron encounters its antiparticle, the electron, and the two are annihilated producing gamma rays. Meanwhile the produced neutron

6

wanders randomly until it is captured by another nucleus which also releases gamma rays (figure 3) (Reines and Cowan, 1994).

Neutrino detection relies upon a container which is filled with a liquid scintillator. In 1950 it was discovered, by several groups, that transparent organic liquids will emit a flash of light when a charged particle or gamma ray passes through them. Though the light flashes are weak their intensity is proportional to the energy of the gamma ray or particle that induces them. A neutrino detector, then, is a large container filled with a transparent organic liquid scintillator, and is surrounded with light detection equipment. The light detection equipment sees the dual flashes of gamma rays produced by positron annihilation and neutron capture during an inverse beta decay event (Reines and Cowan, 1994). Figure 3 is a demonstration of this process.

Previous models delineating geoneutrino production, such as those produced by (Mantovani et al., 2004) or (Enomoto et al., 2007) relied upon bulk compositional estimates of Earth as well of estimates of Uranium, Thorium, and Potassium concentrations. These models then use mass balance equations to determine the distribution of these radioactive elements throughout Earth and therefore an estimation of geoneutrino flux. Figure 4 is a table taken from (Enomoto et al, 2007), to provide a comparison model of crustal composition for use in a geoneutrino model. For more in depth discussion around developing a bulk silicate earth model refer to (Sramek and McDonough et al., 2013).
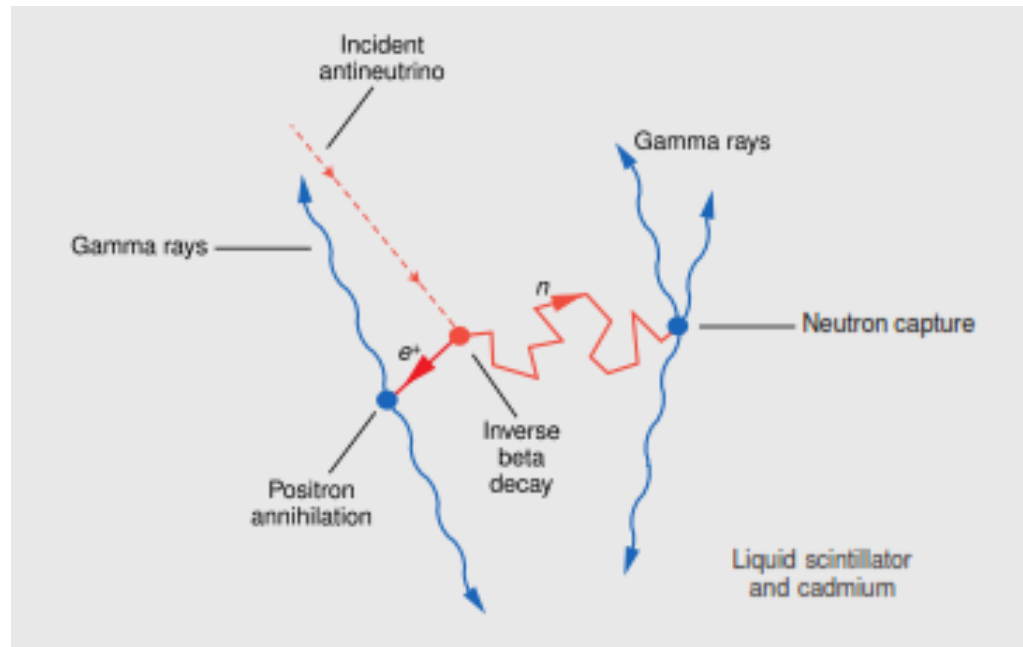
Figure 3. Graphic depiction of inverse beta decay through neutron capture of an incident neutrino. Modified from (Reines and Cowan, 1994).

The reference Earth model

Reservoir		Concentration [ppm]		Mass $\times 10^{16}$ [kg]		Heat production [TW]	
		U	Th	^{238}U	^{232}Th	^{238}U	^{232}Th
Sediment	Continental	2.8	10.7	0.26	0.99	0.26	0.26
	Oceanic	1.7	6.9	0.07	0.28	0.07	0.07
Continental crust	Upper	2.8	10.7	1.85	7.08	1.75	1.86
	Middle	1.6	6.1	1.17	4.47	1.11	1.17
	Lower	0.2	1.2	0.14	0.85	0.13	0.22
Oceanic crust		0.10	0.22	0.04	0.09	0.04	0.02
Mantle	Upper	0.012	0.048	1.28	5.13	1.21	1.35
	Lower	0.012	0.048	3.52	14.1	3.32	3.71
Core	Outer	0	0	0	0	0	0
	Inner	0	0	0	0	0	0
Bulk silicate Earth (BSE)		0.0203	0.0795	8.18	32.1	7.73	8.44

Figure 4. The reference earth model taken from (Enomoto et al., 2007). Geoneutrino flux would be calculated from the bulk composition of each particular layer in this Earth model. The upper continental crust listed in this figure provides a reference model for comparison in terms of uranium and thorium concentration.

The model presented here is a surface geology model of a small area around the Homestake Mine in South Dakota based on collected samples from outcrop. The model targets igneous rocks throughout the northern Black Hills of South Dakota. Igneous rocks were selected due to the incompatible and mobile nature of the radioactive elements of interest: uranium, thorium and potassium. Once rocks have been exposed to erosion forces, the opportunity to lose a significant portion of the radioactive elements is large. Target areas were selected using the USGS geology map of the Black Hills produced by (Redden and DeWitt, 2008). An area was targeted if it provided accessible igneous outcrops that could be found and sampled easily. Many areas were not sampled due to lack of outcrop, access restrictions which may include mine or private ownerships, or being designated as a superfund site.

This model was generated by using gamma ray spectrometer analysis of rock samples throughout the study area. Rock samples were taken to produce a sample of the upper continental crust of interest. Once collected the samples were prepped for crushing by removing any weathering crust that may be present on the sample. Removal of the crust was done using either a rock saw or a rock hammer. Samples were selected for the least amount of weathering before being prepped for cleaning and crushing. These samples were then crushed to fill a uniform volume sixteen ounce paper container before being exposed to a gamma ray spectrometer. The rock crushing machine was set to a 1 cm by 5 cm rectangular opening. A large metal paddle crushes a cleaned rock sample against a metal backing. Once a portion of sample is small enough to pass through the rock crushing opening it is captured in a 16 ounce container. The

spectrometer produces a reading of radioactive decay counts over a set time interval of each individual sample. These radioactive decay count readings were subsequently converted to composition of uranium and thorium measurements in parts per million and potassium measured by percent of total composition. After being compiled the data was then displayed on a map surrounding the area of Lead, South Dakota. The map was populated with data points whose locations were recorded upon collection with a handheld GPS device. Each of these points was then given a value for uranium thorium and potassium based upon the converted spectrometer readouts. Once the map was populated with composition values ESRI's ArcGIS was used to produce an inverse distance weighting interpolation (IDW), based on composition, to fill out three maps displaying uranium, potassium, and thorium concentrations of the study area. A fourth map was created to display neutrino luminosity based upon the method outlined in (Enomoto et al., 2007). The conversion to neutrino luminosity is outlined in equation 3 below.

Equation 3:

$$U^{238}: L_{\bar{V}}\left[\frac{1}{s}\right] = 7.46x10^7 * M[Kg]$$

$$U^{235}: L_{\bar{V}}\left[\frac{1}{s}\right] = 3.2x10^8 * M[Kg]$$

$$Th^{232}: L_{\bar{V}}\left[\frac{1}{s}\right] = 1.62x10^7 * M[Kg]$$

$$K^{40}: L_{\bar{V}}\left[\frac{1}{s}\right] = 2.38x10^8 * M[Kg]$$

Antineutrino luminosity is represented by $L_{\bar{v}}$ in equation 3 which is antineutrino generation per unit time calculated from the samples mass. (Enomoto et al., 2007). Using the natural abundances of each isotope, equation three maybe rewritten to form equation 4, which demonstrates the relation found in natural elements (Enomoto et al., 2007)

Equation 4:

$$U^{nat}: L_{\bar{V}}\left[\frac{1}{s}\right] = 7.64x10^7 * M[Kg]$$

$$Th^{nat}: L_{\bar{V}}\left[\frac{1}{s}\right] = 1.62x10^7 * M[Kg]$$

$$K^{nat}: L_{\bar{V}}\left[\frac{1}{s}\right] = 2.70x10^8 * M[Kg]$$

The antineutrino luminosity numbers produced from these equations for uranium thorium and potassium are combined into a single value for each point. An inverse distance weighting interpolation is, again, applied to produce a map of antineutrino luminosity for the study area. Potassium information is gathered and included in the luminosity maps, however, the current generation of neutrino detectors do not detect geoneutrinos produced by potassium. The energy level produced from potassium neutrinos is below the detection threshold for the current generation of detectors.

CHAPTER III

RESULTS

Tables 1 and 2 found in appendix A are a compilation of the data collected from the study area. "Sample #" is a simple identifier used in the field and lab notes. "Unit" is a rock type classification taken from (Redden and DeWitt, 2008). A list of the rock type classification breakdowns is found in Appendix B "Lat and Long" are the latitudes and longitudes of each collected sample reported in decimal degrees using NAT 83 as the datum." U, Th, and K" are the converted spectrometer values, with U and Th being reported in parts per million, and K being reported in % of sample.

The calculated values of U in ppm, Th in ppm and K in percent were used to create interpolated maps centered on the Homestake Mine of South Dakota. Map 1 demonstrates the distribution of uranium from collected samples in the area. This map highlights an area of increased uranium density in the western portion of the map. One particular sample located within the northwest quadrant of the study area demonstrates a very large uranium value, in comparison to the other collected samples. This value is above 10 ppm uranium, by comparison the average ppm of the upper continental crust is around 2.8 as referenced earlier in figure 4. Map 2 is the inverse distance weighted interpolation (IDW) of the thorium distribution calculated from the collected samples. The thorium distribution also demonstrates an area of increased thorium concentration in the western portion of the study area. This area of increased thorium concentration has a calculated value of parts per million in the 20s. The thorium

concentration found in table 4 lists the average thorium ppm throughout the upper

continental crust as around 10 ppm. A particular sample of rhyolite collected northwest

of the Homestake Mine gave a thorium value of 80 ppm which is well above the average

for rocks in the study area. Map 3 is the interpolated map demonstrating the

concentration of potassium throughout the area. In contrast to the concentration of

thorium and uranium the area of greatest potassium concentration is in the

southeastern portion of the study area. Map 4 is the collective antineutrino luminosity

from uranium, thorium, and potassium. The interpolation of luminosity shows that the

study area is quite luminous, producing the most neutrinos in the eastern and south

eastern sections of the map.
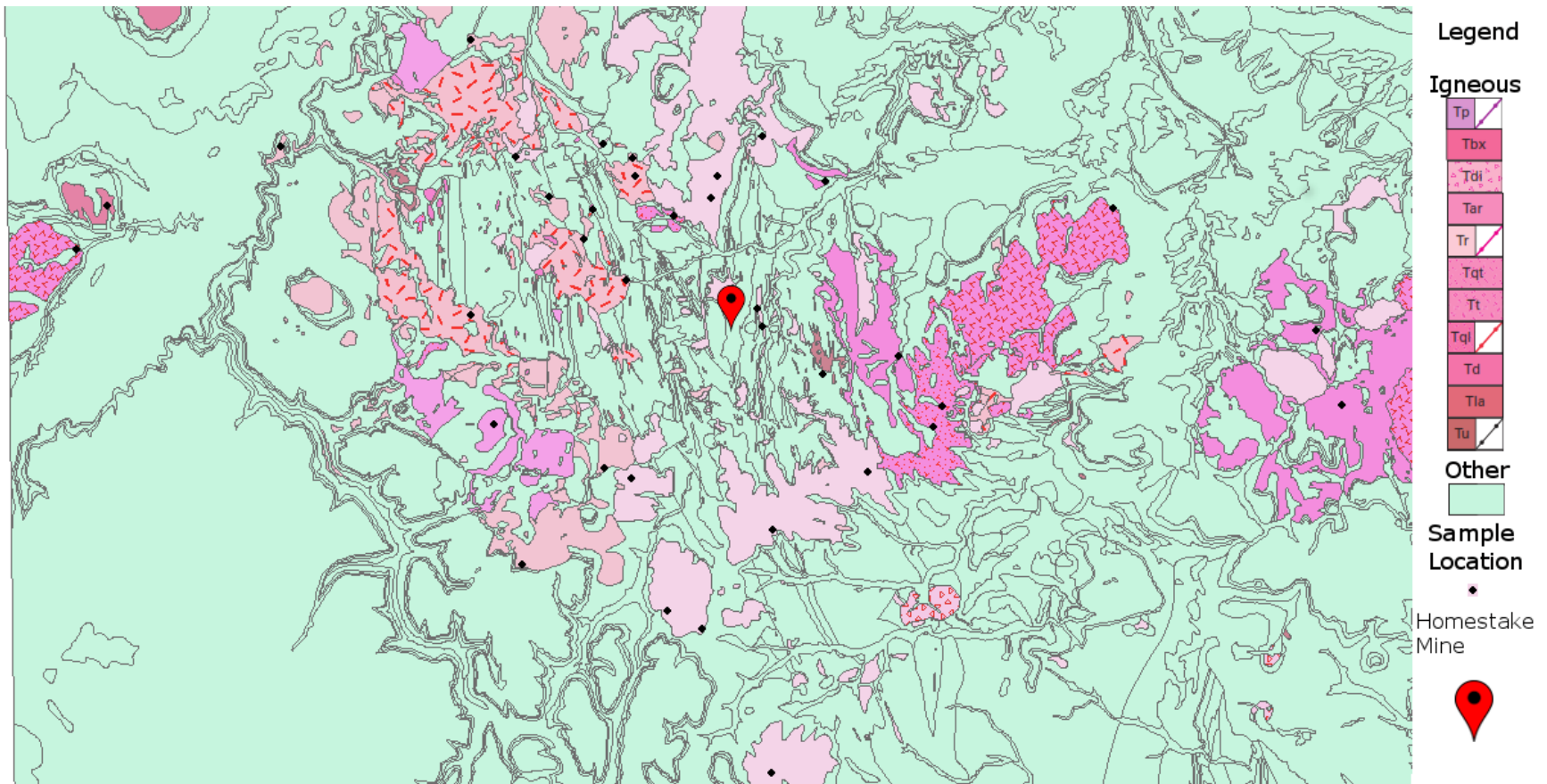
Figure 5. Overview of the study area with data points overlain on a geologic basemap. Igneous units are highlighted. Modified from (Redden and Dewitt, 2008). Red pin indicates the location of the Homestake Mine.

Uranium Parts Per Million (ppm)

Legend

- 0.0 - 1.8
- 1.8 - 2.8 B.S.E.
- 2.8 - 3.5
- 3.5 - 4.7
- 4.7 - 5.9
- 5.9 - 7.0
- 7.0 - 8.2
- 8.2 - 9.4
- 9.4 - 10.5

Miles
0   1.25 2.5   5   7.5   10

1:234,678

Figure 6. Display of an inverse distance weighting (IDW) of uranium parts per million measurements. Each dot represents a sample taken within the area of the Homestake Mine. The Homestake mine is indicated by the red balloon pin.

Thorium Parts Per Million (ppm)

Legend

![dark green]	0 - 10 B.S.E.
![light green]	10 - 20
![pale yellow]	20 - 30
![yellow]	30 - 40
![orange]	40 - 50
![tan]	50 - 60
![brown]	60 - 70
![pink]	70 - 80
![white]	80 - 90

Miles
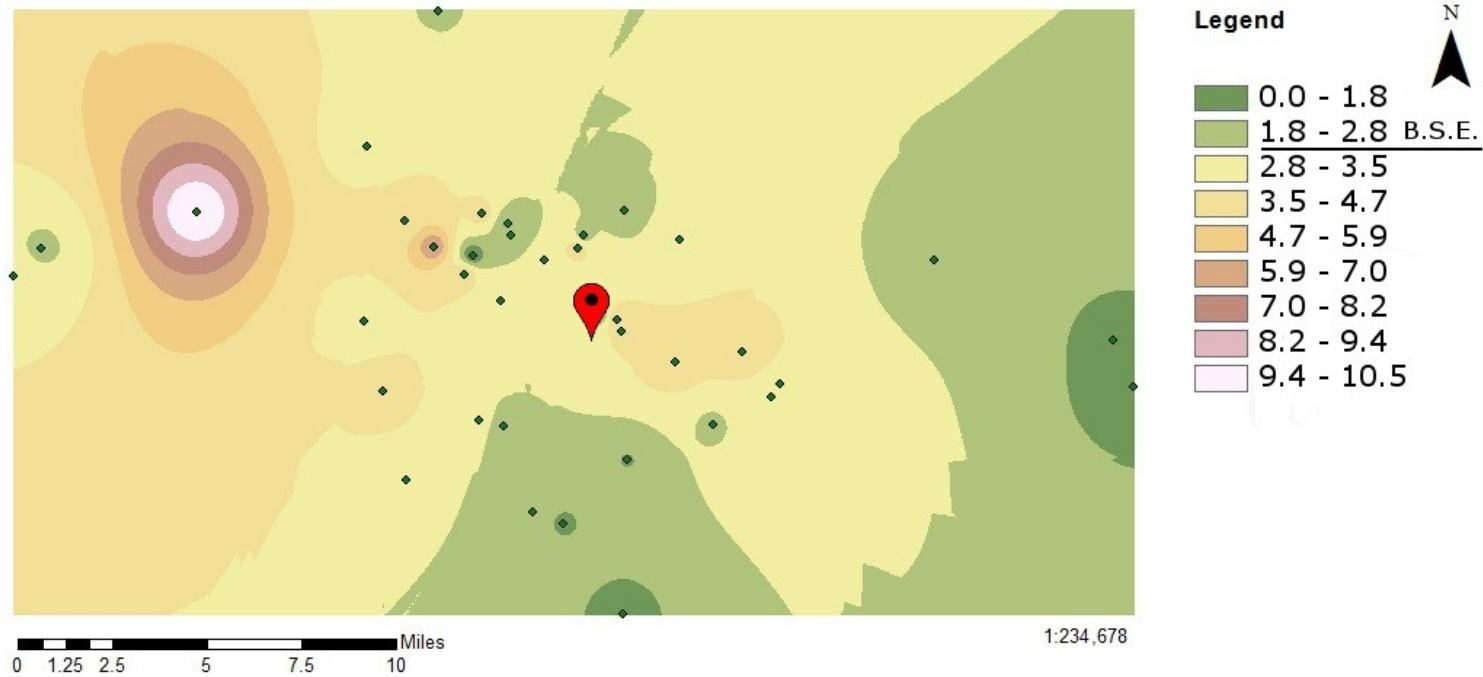0 1.25 2.5   5   7.5   10

1:234,678

Figure 7. Display of an inverse distance weighting (IDW) of thorium parts per million measurements. Each dot represents a sample taken within the area of the Homestake Mine. The Homestake mine is indicated by the red balloon pin.

Figure 8. Display of an inverse distance weighting (IDW) of potassium percent. Each dot represents a sample taken within the area of the Homestake Mine. The Homestake mine is indicated by the red balloon pin.

Figure 9. Display of an inverse distance weighting (IDW) of luminosity. Luminosity is antineutrino generation per unit time (seconds) calculated from the samples mass. (Enomoto et al., 2007). Each dot represents a sample taken within the area of the Homestake Mine. The Homestake mine is indicated by the red balloon pin.
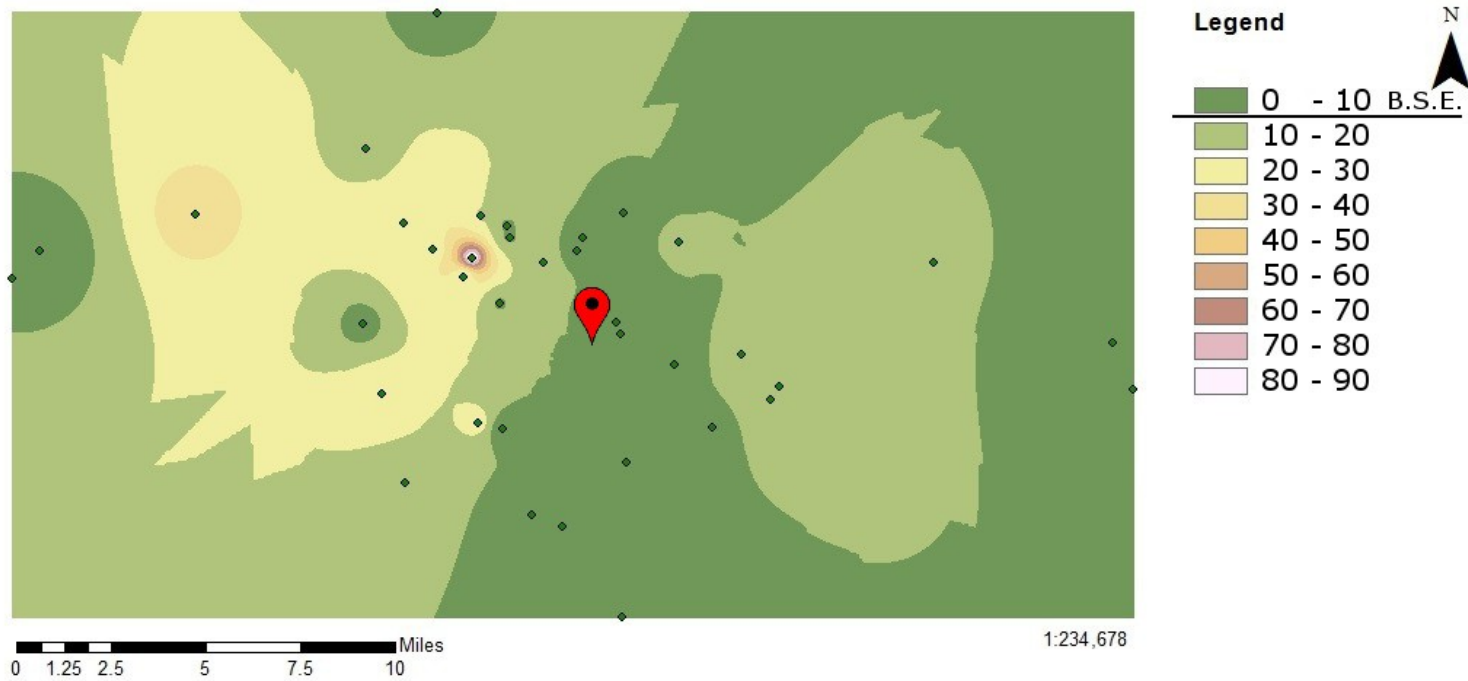
CHAPTER IV

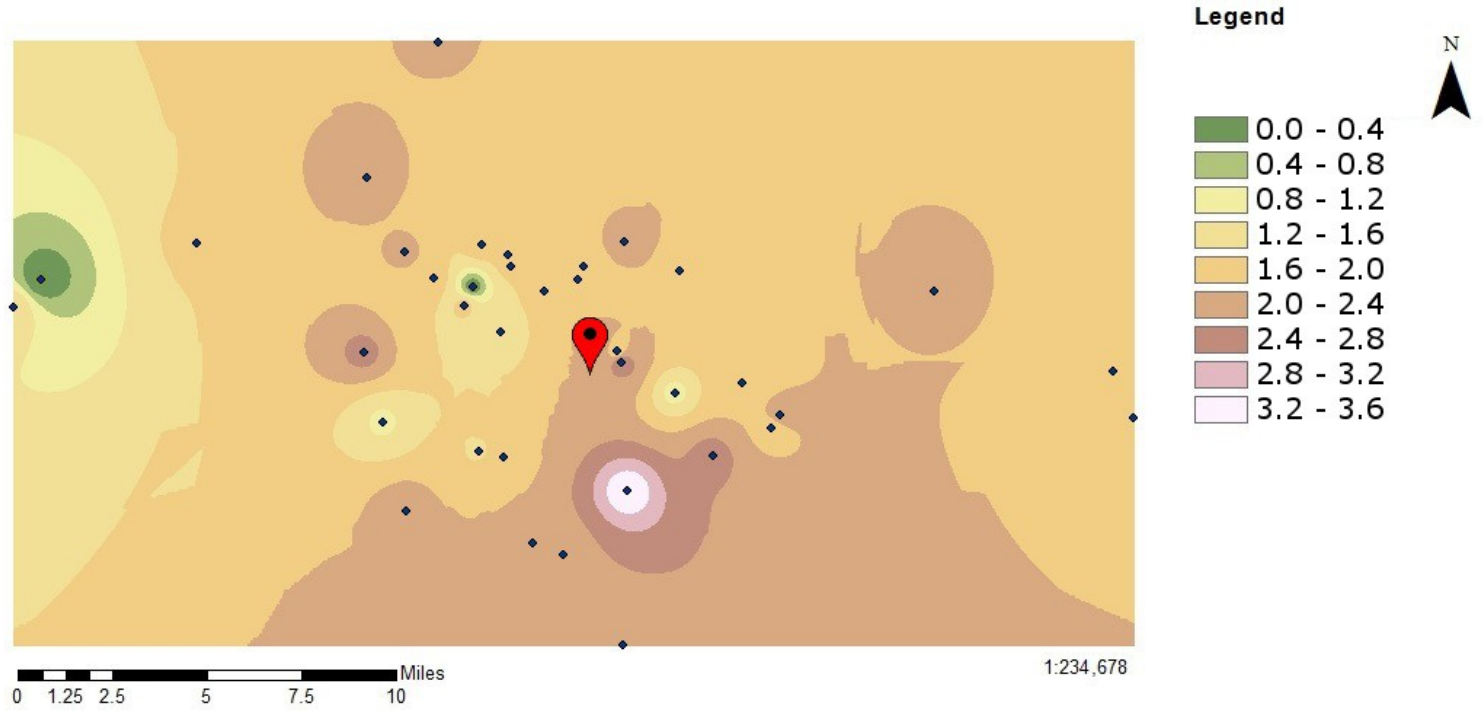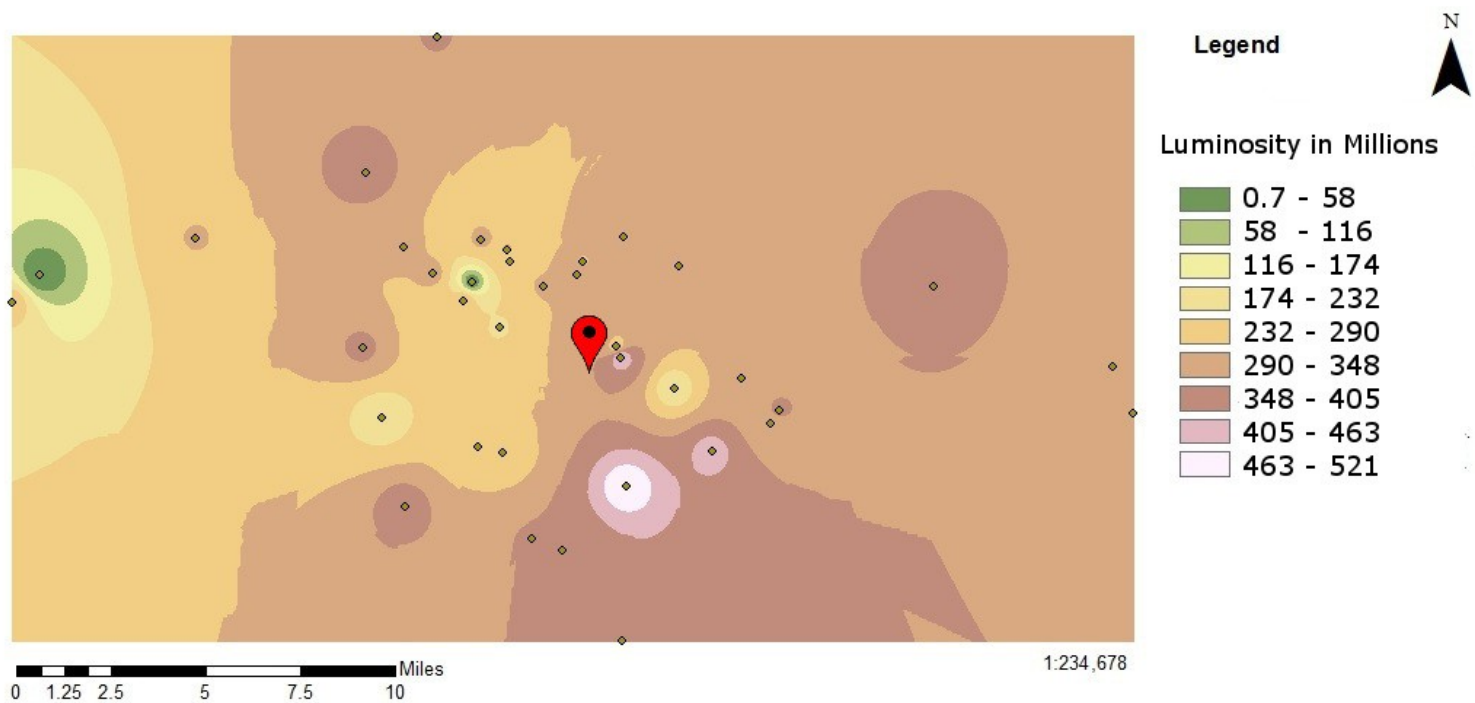## CONCLUSION

The area surrounding the Homestake Mine in South Dakota demonstrates rocks that contain a relatively high amount of uranium and thorium when compared to the bulk silicate Earth model outlined in figure 4. The rocks in the area also contain a large amount of potassium, which is expected from the large amount of felsic igneous rocks found within the Black Hills. The luminosity interpolation map demonstrates a large neutrino flux throughout the entirety of the eastern portion of the study area, and large parts of the western section as well. The rocks collected show an area that is quite radioactive and will produce a locally strong geoneutrino flux for a detector located within the Homestake Mine.

Future work should be concentrated on increasing the data density, and expanding the rock type collection to sedimentary and metamorphic materials This model for geoneutrino flux uses forty data points to create the surface map. Many portions of the study area have a single sample representing a rather large area of igneous rocks, and some areas had to be skipped for logistics or access reasons. The model also only uses igneous rocks while many sedimentary and metamorphic rocks populate the area. More data points would help reduce the bulls-eye effect of having singular points with very high values in comparison to neighboring data points

Data Tables

Table 1

Data table using samples collected in the northern Black Hills. Units uses outcrop designations laid out in table 3. Lattitude and Longitude are reported in decimal degress. Uranium and thorium are reported in parts per million (ppm) and potassium is reported with percent composition by weight

Sample #	Unit	Lat	Long	U	Th	K
BHEZ1	Tla	44.37257	-103.97732	3.26	10.69	1.57
BHEZ2	Tql	44.38312	-103.9667	2.08	0.81	0.00
BHEZ3	Tp	44.39708	-103.90717	10.54	36.29	1.67
BHEZ4	Tp	44.4222	-103.84194	2.78	17.59	2.25
BHEZ5	Tr	44.39649	-103.79756	4.32	20.14	1.94
BHEZ6	Tqt	44.39275	-103.78749	1.51	9.06	1.68
BHEZ7	Tqt	44.38843	-103.78675	1.06	9.00	1.74
BHEZ8	Tp	44.38058	-103.80108	0.00	89.71	0.00
BHEZ9	Tp	44.38363	-103.81619	7.04	25.26	1.92
BHEZ10	Tr	44.39359	-103.82715	4.06	21.17	2.11
BHEZ11	Tqt	44.35524	-103.84319	3.27	7.83	4.54
BHEZ12	Tr	44.47446	-103.81455	2.27	3.69	2.05
BHEZ13	Td	44.38673	-103.72179	3.30	12.74	1.91
BHEZ14	Tr	44.39774	-103.74316	1.33	4.40	2.17
BHEZ15	Tr	44.38832	-103.75843	1.86	7.92	1.73
BHEZ16	Tr	44.38291	-103.76107	4.26	8.02	1.85
BHEZ17	Tt	44.37869	-103.7738	3.16	12.79	1.78
BHEZ18	Tt	44.37316	-103.80419	4.53	20.66	1.76

Table 2

Data table using samples collected in the northern Black Hills. Assumed units uses outcrop designations laid out in table 3. Lattitude and Longitude are reported in decimal degress. Uranium and thorium are reported in parts per million (ppm) and potassium is reported with percent composition by weight.

Sample #	Unit	Lat	Long	U	Th	K
BHEZ19	Tqt	44.36298	-103.79033	2.74	9.51	1.38
BHEZ20	Tr	44.35572	-103.74575	4.74	7.93	1.55
BHEZ21	Tr	44.35745	-103.75236	1.32	6.96	2.25
BHEZ22	Tp	44.31751	-103.79874	3.40	24.86	1.51
BHEZ23	Tr	44.31479	-103.78926	1.24	3.24	1.89
BHEZ24	Tar	44.32856	-103.83578	4.51	28.58	1.09
BHEZ25	Tp	44.29423	-103.82697	3.00	16.52	2.26
BHEZ26	Tr	44.28232	-103.77791	1.75	4.97	2.03
BHEZ27	Tr	44.27783	-103.76631	1.06	5.59	2.22
BHEZ28	Tr	44.30191	-103.74166	1.14	6.97	3.57
BHEZ29	Tr	44.35151	-103.74403	3.65	9.16	2.82
BHEZ30	Tu	44.33964	-103.72364	4.48	9.47	1.01
BHEZ31	Tr	44.31536	-103.70915	2.11	6.58	2.60
BHEZ32	Tt	44.32616	-103.68659	3.00	16.93	1.79
BHEZ33	Tt	44.3312	-103.68334	3.42	17.99	2.12
BHEZ34	Tr	44.2427	-103.74354	0.79	5.34	2.18
BHEZ35	Td	44.34369	-103.69779	4.38	11.10	1.67
BHEZ36	Tql	44.37881	-103.62429	1.20	11.07	2.06
BHEZ37	Td	44.3482	-103.55552	1.04	7.36	1.63
BHEZ38	Tp	44.33008	-103.54734	0.67	8.52	1.87
BHEZ39	Xh	43.84508	-103.57732	0.65	0.32	1.57

APPENDIX B

Unit Designations

Table 3

Unit designations and descriptions modified from (Redden and DeWitt, 2008).

Designation	General Description	Age
TP	Phonolitic Intrusive Rocks	Eocene to Paleocene
Tbx	Tertiary iintrusion breccias	Eocene to Paleocene
Tdi	Breccia and layered tuffaceous unit	Eocene to Paleocene
Tr	Rhyolitic intrusive rocks	Eocene to Paleocene
Tqt	Quartz trachytic intrusive rocks	Eocene to Paleocene
Tt	Trachytic intrusive rocks	Eocene to Paleocene
Tql	Quartz latitic intrusive rocks	Eocene to Paleocene
Tdi	Dacitic intrusive rocks	Eocene to Paleocene
Tu	Tertiary intrusive rocks	Eocene to Paleocene

REFERENCES

"About Us," *Sanford Underground Research Facility*, accessed February 15th, 2014

   http://sanfordlab.org/about/deep-science-frontier-physics.

Bachall, John N. Davis, Raymond Jr. and Wolfenstein, Lincoln (1988) Solar neutrinos: a field in

   transition. *Nature.* 334, 487 – 493.

Bethe, H. A. and Bacher, R. F. (1936) Disintegration and nuclear Forces. *Review of Modern*

   Physics 8 (82): 184.

Enomoto, S., Ohtani, E., Inoue, K., & Suzuki, A. (2007). Neutrino geophysics with KamLAND and

   future prospects. *Earth and Planetary Science Letters, 258*(1-2), 147-159.

Lesko, Kevin. (2013) Why the US Needs a Deep Domestic Research Facility: Owning rather than

   Renting the Education Benefits, Technology Advances, and Scientific Leadership of

   Underground Physics. *Sanford Underground Research Facility*

   http://sanfordlab.org/lbnl/1428.

Mantovani, F., Carmignani, L. Fiorentini, G. and Lissia, M. (2004). Antineutrinos from Earth: A

   reference model and its uncertainties, *Phys. Rev. D, 69*, 013001.

Redden, J. A., DeWitt, E., Berry, J., Bowles, C. G., Braddock, W. A., Cattermole, C. M., . . .

   Zartman, R. E. (2008). *Maps showing geology, structure, and geophysics of the central*

   black hills, south dakota U. S. Geological Survey.

Reines, Frederick and Cowan, Clyde Jr. (1997) The Reines-Cowan Experiments Detecting the

Poltergeist: A compilation of papers and notes by Fred Reines and Clyde Cowan. *Los*

Alamos Science November 25.

Sramek, O., McDonough, W. F., Kite, E. S., Lekic, V., Dye, S. T., & Zhong, S. (2013). Geophysical

and geochemical constraints on geoneutrino fluxes from earth's mantle. *Earth and*

Planetary Science Letters, 361, 356-366.